Neutral Red Film Augments Direct and Mediated Extracellular Electron Transfer Performed by *Clostridium pasteurianum* DSM 525

Ana Clara Bonizol Zani , João Carlos de Souza , Adalgisa Rodrigues de Andrade , Valeria Reginatto *

Posted Date: 10 September 2024

doi: 10.20944/preprints202409.0776.v1

Keywords: *Clostridium pasteurianum* DSM 525; glycerol; mediated electron transfer (MET); neutral red (NR); methyl viologen (MV)

 doi:10.20944/preprints202409.0776.v1

Article

Neutral Red Film Augments Direct and Mediated Extracellular Electron Transfer Performed by *Clostridium pasteurianum* DSM 525

Ana Clara Bonizol Zani [1], João Carlos de Souza [1,2], Adalgisa Rodrigues de Andrade [1,2] and Valeria Reginatto [1,*]

[1] Department of Chemistry, Faculty of Philosophy, Sciences and Letters at Ribeirão Preto (FFCLRP), University of São Paulo (USP), Ribeirão Preto CEP 14040-901, SP, Brazil
[2] São Paulo State University (UNESP), Institute of Chemistry, National Institute for Alternative Technologies of Detection, Toxicological Evaluation and Removal of Micropollutants and Radioactives (INCT-DATREM), Araraquara CEP 1480-900, SP, Brazil
* Correspondence: valeriars@ffclrp.usp.br

Abstract: Extracellular electron transfer (EET) is key to the success of microbial fuel cells (MFCs). *Clostridium* sp. often occurs in MFC anode communities, but its ability to perform EET remains controversial. We have employed *Clostridium pasteurianum* DSM 525 as biocatalyst in a glycerol-fed MFC, designated MFC$_{DSM}$. We have also followed the EET of this biocatalyst in the presence of a mediator, namely soluble neutral red (NR), soluble methyl viologen (MV), neutral red film (FNR), or methyl viologen film (FMV). MFC$_{DSM}$ provided power and current densities (j) of 0.39 μW.cm^{-2} and 2.47 μA.cm^{-2}, respectively, which evidenced that the biocatalyst performs direct electron transfer (DET). Introducing 150.0 μM NR or MV into the MFC$_{DSM}$ improved the current density by 7.0- and 3.7-fold (17.05 and 8.45 μA.cm^{-2}), respectively. After 20 cyclic voltammetry (CV) cycles, the presence of FNR in the MFC$_{DSM}$ anodic chamber provided almost twofold higher current density (30.76 μA.cm^{-2}) compared the presence of NR in the MFC$_{DSM}$. Introducing MV or FMV into the MFC$_{DSM}$ anodic chamber gave practically the same current density after 10 CV cycles. The MFC$_{DSM}$ anodic electrode might interact with FMV weakly than with FNR, so FNR is more promising to enhance *C. pasteurianum* DSM 525 EET within MFC$_{DSM}$.

Keywords: *Clostridium pasteurianum* DSM 525; glycerol; mediated electron transfer (MET); neutral red (NR); methyl viologen (MV)

1. Introduction

The increasing world population has raised energy consumption substantially and motivated the search for cleaner and sustainable technologies [1]. In this context, several studies have attempted to improve bioelectrochemical systems (BESs), including microbial fuel cells (MFCs), to attain energy. Investigating new biocatalysts and modifying electrodes is fundamental to enhance microorganism-electrode interaction and to optimize extracellular electron transfer (EET), which are essential for further developing BESs [1].

MFCs recognizably produce clean energy while simultaneously degrading organic compounds and pollutants [2]. Nowadays, this technology is mostly applied by using mixed cultures or microbial consortia. However, there is a gap in the knowledge about how some microorganisms, especially Gram-positive bacteria, contribute to generating energy in MFCs and their actual EET capacity [3].

Shewanella sp. and *Geobacter* sp. have been extensively studied as pure cultures in MFCs [3,4]. Given that mixed cultures typically encompass numerous genera, the dominance of these species has prevented the electroactivity of other microorganisms from being explored. Furthermore, although Gram-positive bacteria are widely present in bioanodes, their electrogenic capacity has been poorly investigated. Compared to Gram-negative bacteria, Gram-positive bacteria have thicker cell wall, which may reduce their electron transfer efficiency [5]. This may be the reason why the EET of Gram-positive bacteria has been less frequently researched.

 doi:10.20944/preprints202409.0776.v1

Species belonging to the genus *Clostridium* often occur in microbial communities of MFC bioanodes, and they act mainly as fermenter [3,6–8]. However, the EET ability of *Clostridium* sp. remains poorly explored. By using cyclic voltammetry, in 2014 Choi et al. identified redox peaks for *C. pasteurianum* DSM 525, which highlighted its significant electroactivity. The authors discussed the asymmetry of the reduction and oxidation peaks, which was comparable to the asymmetry observed in current-producing electroactive microorganisms [9].

EET can occur through direct electron transfer (DET) or mediated electron transfer (MET) [10,11]. Microorganisms that exhibit DET frequently contain redox proteins in their outer membrane, so they transfer electrons directly from these redox-active centers to the electrode. Nevertheless, some microorganisms that lack DET can carry out MET through redox mediator molecules [10]. For instance, *Pseudomonas aeruginosa* and *Shewanella oneidensis* are known for their ability to excrete phenazines and flavins, respectively, which can serve as electron mediators and enhance EET [12,13].

To improve EET, exogenous electron redox shuttles (mediators) can be added alongside microorganisms exhibiting low EET efficiency. The choice of mediator is critical, and criteria such as biological compatibility, stability, and redox potential should be considered [1,14]. At non-toxic concentrations, soluble neutral red (NR), a phenazine-based molecule, and soluble methyl viologen (MV), a viologen-based molecule, can mediate electron transfer [1,15]. Additionally, they provide fast electrochemical responses and efficiently operate at negative potentials, fulfilling the aforementioned criteria.

Herein, we have assessed the ability of the Gram-positive *Clostridium pasteurianu*m strain DSM 525 to act as an electroactive biocatalyst in the anodic chamber of a glycerol-fed MFC, designated MFC_{DSM}. We will show that this bacterial strain can perform EET. We will also show that adding NR or MV in solution or as a film (FNR and FMV, respectively) to the MFC_{DSM} anodic chamber, especially FNR, improves the MFC_{DSM} performance and results in higher current densities.

2. Materials and Methods

2.1. Bacterial Cell Growth and Culture Medium

Clostridium pasteurianum DSM 525 was obtained from the culture collection of *Deutsche Sammlung von Mikroorganismen und Zellkulturen.* The bacterial cells were maintained in glycerol solution (20%, w v^{-1}) at -80 °C, in a freezer.

Before the electrochemical tests were conducted, the cells were activated in fresh *Reinforced Clostridium Medium* (RCM, Sigma-Aldrich). After that, the cells were transferred to a pre-inoculum culture medium (the same medium used in the electrochemical tests) at 35 °C for 15 h. The medium that was used in the tests has been described by Lovley and Phillips (LP medium) and comprises (in mmol L^{-1}) 28.0 NH_4Cl, 0.50 $MgCl_2{\cdot}6H_2O$, 0.40 $MgSO_4{\cdot}7H_2O$, 0.68 $CaCl_2{\cdot}2H_2O$, 1.30 KCl, 1.70 NaCl, 0.003 $NaMoO_4{\cdot}2H_2O$, 30.0 $NaHCO_3$, 5.20 Na_2PO_4, and 4.30 $NaH_2PO_4{\cdot}H_2O$, supplemented with 0.05 g L^{-1} yeast extract [16]. Glycerol at 1.0 g L^{-1} was added as carbon source. The tests were carried out under anaerobic conditions (N_2 was purged through the medium for 8 min before the tests were initiated); the initial was pH 7.0 (25 ± 2 ºC). The sterility of the culture medium and materials was ensured by autoclaving them at 121 °C and 1 atm for 20 min.

Before *C. pasteurianum* DSM 525 was directly exposed to 150.0 μM NR or MV, O.D. at 600 nm was measured to verify whether there were any inhibitory effects. Initially, the bacterial cells were activated in RCM medium and incubated for 24 h. Subsequently, they were transferred to LP medium, at an initial O.D. of 0.1, in the presence of 150.0 μM NR or MV. Later, O.D. was measured after bacterial growth for 16 h.

2.2. Glycerol-Fed C. pasteurianum DSM 525-Based MFC Setup (MFC_{DSM})

MFC_{DSM} consisted of a double-chamber setup, namely an anodic chamber (36 mL) and a cathodic chamber, connected by an external resistance of 1000 Ω. The anodic chamber was filled with LP medium (pH 7.0) and inoculated with *C. pasteurianum* DSM 525 (O.D. at 600 nm = 0.2). The anode material was carbon cloth (2.0 x 2.5 cm), and the cathode (open-air cathode) was made of carbon cloth

 doi:10.20944/preprints202409.0776.v1

with 40% platinum (A6ELAT/BASF), hot-pressed with a Nafion® membrane (NRE-212/Sigma-Aldrich) at 130 °C and 35 kgf cm^{-2} for 180 s [17]. All the electrochemical measurements are referenced to the $Ag/AgCl_{(sat)}$ electrode. After inoculation, *C. pasteurianum* DSM 525 remained in the MFC for 18 h to ensure that MFC_{DSM} was active for the electrochemical tests to be conducted.

2.3. Electrochemical Measurements in MFC_{DSM}

To assess how C. pasteurianum DSM 525 performed in MFC_{DSM}, polarization/power curves and electrochemical impedance spectroscopy (EIS) were carried out in an AUTOLAB PGSTAT 30 potentiostat/galvanostat (NOVA 2.1 software).

Initially, the polarization curves were obtained at a low scan rate (1 mV s^{-1}) starting from the open circuit potential (OCP) down to zero. OCP denotes the maximum operating voltage of the system, where the current is zero [18]. MFC_{DSM} operated without an external resistance until OCP stabilized. Subsequently, the power curve was derived from the polarization curves according to equation 1.

$$P = \frac{i\,U}{A} \quad (1)$$

where "P" is the power density (W m^{-2}), "i" is the current (A), "U" is the voltage (V), and "A" is the anode geometric area (m^2).

EIS was performed at OCP, from 100 kHz to 0.01 Hz. Ten frequency points per decade with a root mean square (r.m.s.) sinusoidal perturbation were employed; the amplitude was 10 mV.

2.4. NR or MV as Mediator

NR or MV was introduced into the MFC_{DSM} anodic chamber to verify whether they promoted *C. pasteurianum* DSM 525 EET. Specifically, 4 g L^{-1} NR or 5 g L^{-1} MV, prepared in 0.025 M K_2HPO_4/KH_2PO_4 buffer (pH = 7.0) in 0.10 M KNO_3, was added to the MFC_{DSM} anodic chamber.

The kinetic study was conducted in LP medium (support electrolyte); a 50-mL single-chamber cell was employed. The electrochemical cell included three electrodes: a carbon cloth (2.0 x 2.5 cm) as working electrode, $Ag/AgCl_{(sat)}$ as reference electrode, and a platinum wire as counter electrode. All the solutions were deaerated with N_2 gas. Kinetics was monitored by cyclic voltammetry (CV) at various scan rates, from 1 to 50 mV s^{-1}, for 100 µM NR or 200 µM MV. An AUTOLAB PGSTAT 30 potentiostat/galvanostat (NOVA 2.1 software) was used. The potential window ranged from -0.9 to -0.1 V *vs* $Ag/AgCl_{(sat)}$ and -1.1 to 0.2 V *vs* $Ag/AgCl_{(sat)}$ for NR and MV, respectively.

2.5. FNR or FMV Deposition on the MFC_{DSM} Anode

FNR or FMV was deposited on the MFC_{DSM} anode according to the methodology described by Ghica and Brett [19]. The same electrochemical cell employed in section 2.4 was used. All the solutions were deaerated with N_2 gas.

To obtain the MFC_{DSM} anode modified with FNR, first a 0.025 M K_2HPO_4/KH_2PO_4 buffer solution (pH = 6) was prepared in 0.10 M KNO_3 containing 1 mM NR. The film was formed by conducting CV from -1.0 to 1.3 V *vs* $Ag/AgCl_{(sat)}$ at 50 mV s^{-1}. Different numbers of cycles (10, 15, 20, or 30) were evaluated.

The MFC_{DSM} anode modified with FMV was prepared under similar conditions. First, a 0.025 M K_2HPO_4/KH_2PO_4 buffer solution (pH = 7) in 0.10 M KNO_3 containing 1 mM MV was prepared. Then, CV was carried out from -1.1 to 0.2 V *vs* $Ag/AgCl_{(sat)}$ at 50 mV s^{-1}. The number of cycles (10, 15, 20, or 30) was evaluated, as well.

EIS was performed to compare the internal resistance of the unmodified MFC_{DSM} anode with the internal resistance of the MFC_{DSM} anode modified with FNR or FMV. Frequency ranges from 100 kHz to 0.01 Hz and ten frequency points per decade with a root mean square (r.m.s.) sinusoidal perturbation were employed; the amplitude was 10 mV. For the unmodified MFC_{DSM} anode, OCP was used; for the MFC_{DSM} anode modified with FNR or FMV, the potential was -0.22 V or -0.16 V *vs* $Ag/AgCl_{(sat)}$, respectively.

 doi:10.20944/preprints202409.0776.v1

CVs were also run for the MFC anode modified with FNR or FMV in the presence and absence of *C. pasteurianum* DSM 525. The potential window of -0.9 to -0.1 V *vs* Ag/AgCl$_{(sat)}$ was used for *C. pasteurianum* DSM 525 and FNR, 20 cycles, whereas the potential window of -1.1 to 0.2 V *vs* Ag/AgCl$_{(sat)}$ was employed for *C. pasteurianum* DSM 525 and FMV, 10 cycles.

2.6. Electrochemical Setup and Measurements Obtained by Using C. pasteurianum DSM 525 Alone or in the Presence of NR, MV, FNR, or FMV

The electrochemical measurements were conducted by using the electrochemical cell setup detailed in section 2.4. Amperometric i-t tests were performed to evaluate the current density of C. pasteurianum DSM 525 under various conditions: in the absence of a mediator (control), in the presence of NR or MV, and in the presence of FNR or FMV. These measurements were carried out at a constant potential for 960 s. An anodic overpotential (η) of 250 mV was applied for both mediators. Specifically, tests regarding NR were subjected to -0.22 V vs Ag/AgCl$_{(sat)}$, while tests involving MV were maintained at a constant potential of -0.16 V vs Ag/AgCl$_{(sat)}$. The current density was obtained at the end of the amperometric i-t test at 960 s.

Initially, 20.0, 50.0, 75.0, 100.0, or 150.0 µM NR or MV was evaluated in LP medium at pH 7.0 (25 ± 2 °C). As for the tests involving FNR or FMV, four CV cycles were employed to obtain the film deposited on the anode. The methodology outlined in section 2.4 was followed. Subsequently, the anode was transferred to fresh LP medium at pH 7.0 (25 ± 2 °C). Before each test, the solutions were deaerated with N_2.

For the tests involving C. pasteurianum DSM 525 and NR, MV, FNR, or FMV, DSM 525 was initially activated in RCM medium. After bacterial growth, the cells were transferred to a pre-inoculum containing LP medium, where it remained for 15 h. Then, an aliquot was transferred to another LP medium and incubated for 18 h. The bacterial cell culture was standardized to an O.D. at 600 nm of 0.20. After the O.D. was standardized, the supernatant was removed by centrifugation at 7000 rpm for 5 min and discarded. The resulting cell pellet was added to the assays containing 150.0 µM NR or MV and to the assays containing FNR or FMV in all cycles.

3. Results and Discussion

3.1. C. pasteurianum Electroactivity in MFC$_{DSM}$

Figures 1A and B respectively show the power/polarization and EIS curves recorded for *C. pasteurianum* DSM 525 operating in an MFC added with 1 g L^{-1} glycerol (MFC$_{DSM}$).

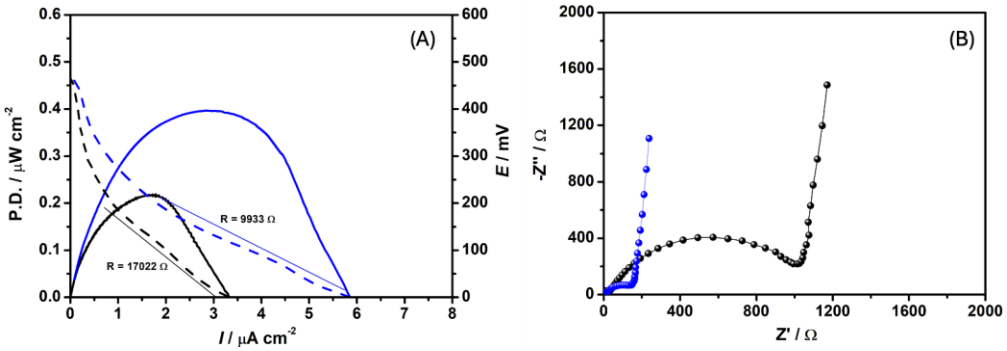

Figure 1. (A) Power and polarization curves of the glycerol-fed MFC with *C. pasteurianum* DSM 525 as biocatalyst (MFC$_{DSM}$-blue line) and without the biocatalyst (abiotic control-black line). (B) EIS spectra obtained for MFC$_{DSM}$ (blue dots) and the abiotic control (black dots) in 1.0 g L^{-1} glycerol at OCP.

The maximum power achieved with MFC$_{DSM}$ and the abiotic control was 0.39 and 0.22 µW cm^{-2}, respectively. The maximum current density achieved with MFC$_{DSM}$ and the abiotic control was 3.02 and 1.72 µA cm^{-2}, respectively. In other words, the current density almost doubled in the presence of

 doi:10.20944/preprints202409.0776.v1

C. pasteurianum DSM 525, indicating that this biocatalyst can perform direct EET to the electrode, effectively transferring electrons through the external circuit.

Although the genus *Clostridium* is typically known for its fermentative ability, it has also been demonstrated to transfer electrons to electrodes through ferredoxin-mediated processes [20]. However, the electroactive activity of *C. pasteurianum* remains considerably limited and poorly understood. Only in 2014 did Choi et al. suggest that *C. pasteurianum* is electroactive. These authors showed that *C. pasteurianum* DSM 525 can use both the electrode and substrate (glycerol and glucose) as electron donors through DET in a BES. By employing CV, the authors observed well-defined but asymmetric redox peaks for *C. pasteurianum* DSM 525, which indicates a quasi-reversible reaction. The authors highlighted similarities between these asymmetric peaks and the peaks observed for other electroactive microorganisms that can reduce Fe (III) and produce current [9].

Furthermore, the polarization curves obtained for MFC_{DSM} and the abiotic control showed about 1.7-fold lower MFC internal resistance in the former case (9933 and 17022 Ω, respectively). Polarization curves are a valuable tool to understand how an MFC behaves because they allow the main domains of potential losses limiting performance to be identified [21,22].

Also, we used EIS to describe how MFC_{DSM} and the abiotic control behave. We conducted the EIS tests at OCP (MFC_{DSM} = -0.265 V; abiotic control = -0.331 V *vs* $Ag/AgCl_{(sat)}$). From these values, we generated a Nyquist plot (Figure 1B), which provided information about the resistance of the solution (R_s), namely 96.30 and 16.10 Ω for MFC_{DSM} and the abiotic control, respectively. We attributed the higher Rs obtained for MFC_{DSM} to the presence of microorganisms in the solution [23].

Additionally, total impedance (R_{ct}), which is associated with the charge transfer process, was 17-fold lower for MFC_{DSM} compared to the abiotic control (65 and 1128 Ω, respectively). This indicated that *C. pasteurianum* DSM 525 enhanced the efficiency of the overall electron transfer process. At low frequencies, a straight line characteristic of limited diffusion processes arose [23]. Moreover, the double layer capacitance (C_{dl}) of MFC_{DSM} was 2.2-fold higher (C_{dl} = 3.8 μF cm^{-2}) compared to the abiotic control (C_{dl} = 1.7 μF cm^{-2}). *C. pasteurianum* DSM 525 present on the electrode probably helped to increase C_{dl}.

3.2. NR and MV Electrochemical Characterization

Figures 2A and B respectively show the electrochemical behavior of NR and MV in LP medium in the presence of glycerol (1 g L^{-1}) at pH 7.0.

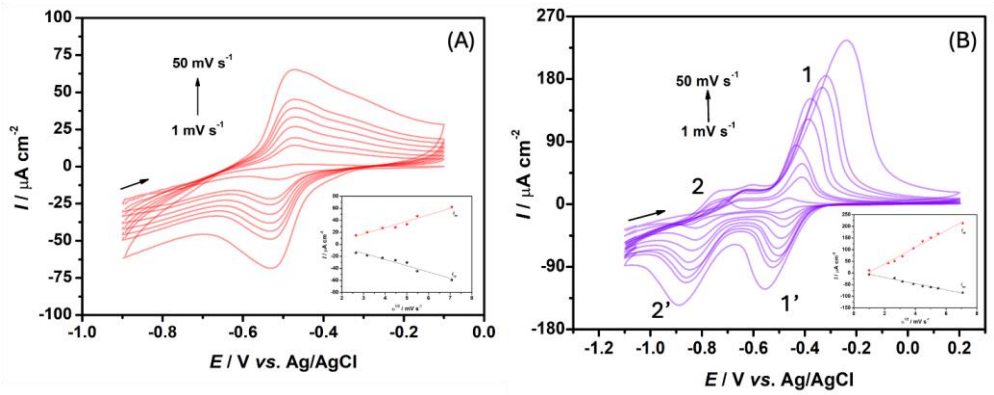

Figure 2. Cyclic voltammograms (CVs) of (A) 100 μM NR and (B) 200 μM MV in LP medium at pH 7.0 (25 ± 2 °C). CVs recorded as a function of the scan rate. Inserted graph: anodic (I_{ap}) and cathodic (I_{cp}) current peaks plotted as a function of the square root of the scan rate.

NR is a phenazine-type molecule bearing a nitrogen-heterocyclic ring in its structure [24]. As mentioned earlier, many microorganisms lack redox-active proteins for DET on their cell surfaces, but they can perform MET by producing their own mediators, such as pyocyanin [12]. Alternatively, molecules of this class, which have well-known redox properties, can be added as mediators in BESs [19].

 doi:10.20944/preprints202409.0776.v1

Figure 2A displays the CV curves obtained for 100.0 µM NR at different scan rates. A redox couple centered around -0.47 and -0.53 V *vs* Ag/AgCl(sat) emerged. Pauliukaite et al. (2016) studied the formation of poly(neutral red) films and reported a pair of redox peaks centered at -0.6 and -0.5 V *vs* SCE, in phosphate buffer, which they attributed to NR-leuco–NR reduction–oxidation processes [25].

Furthermore, CV measurements at various scan rates ranging from 1 to 50 mV s^{-1} provided insights into the electrochemical behavior of NR. I_{ap} was linearly related with the square root of the scan rate, described by the equation: $I_{ap} = 5.3290\ x\ 10^{-4}v - 7.4421\ x\ 10^{-4}$ (R^2 = 0.9514). Similarly, I_{cp} increased linearly with the square root of the scan rate, following the equation: $I_{cp} = -5.1927\ x\ 10^{-4}v - 8.1165\ x\ 10^{-4}$ (R^2 = 0.9409). This response, shown in the graph inserted in Figure 2A, indicated a diffusion-controlled process [26].

Overall, the electrochemical behavior of NR in LP medium closely resembled the way it behaves in supporting electrolytes such as phosphate buffer solutions [25], MOPS buffer with 10 mM $MgCl_2$ and 100 mM glucose [24].

MV, a viologen-based mediator, plays a significant role as electron relay. It exhibits rapid electrochemical response at negative potentials, which allows it to be applied in diverse areas such as batteries and as a redox mediator in numerous enzymatic reactions [15,27]. Moreover, in other applications, MV has been shown to redirect the electron flow from *Clostridium acetobutylicum* by controlling the NADH/NAD^+ balance [28].

MV displays three main oxidation states [29]. Figure 2B depicts the CVs recorded for 200 µM MV at scan rates ranging from 1 to 50 mV s^{-1}. The CV curves exhibited two redox pairs: one at -0.41 and -0.48 V *vs* Ag/AgCl(sat), denoted 1 and 1', respectively, and another at -0.65 and -0.83 V *vs* Ag/AgCl(sat), denoted 2 and 2', respectively. According to Shpilevaya and Foord, reduction peak 1' corresponds to MV^+ formation, which is consistent with reaction 2. Reduction peak 2' refers to formation of the neutral molecule in MV^0 solution (reaction 3). The oxidation peaks labelled 2 and 1 correspond to reactions 4 and 5, respectively [29]

Reaction 2: $MV^{2+} + e^- \rightarrow MV^+\ (peak\ 1')$

Reaction 3: $MV^+ + e^- \rightarrow MV^0\ (peak\ 2')$

Reaction 4: $MV^0 \rightarrow MV^+ + e^-(peak\ 2)$

Reaction 5: $MV^+ \rightarrow MV^{2+} + e^-\ (peak\ 1)$

Generally, MV^{2+} undergoes reduction through a reversible reaction involving an electron, to give a blue cation radical. This radical can undergo further reduction to its neutral form (MV^0), which typically adsorbs onto the electrode surface [27].

The graph inserted in Figure 2B shows the profile of I_{ap} and I_{cp} *vs* the square root of the scan rate for the redox couple 1/1'. I_{ap} behaved according to the equation: $I_{ap} = 0.001790\ v - 0.001666$ (R^2 = 0.984317), while I_{cp} followed the equation: $I_{cp} = -6.68305\ x\ 10^{-4}v + 3.653847\ x\ 10^{-4}$ (R^2 = 0.979345). The linear increase suggested diffusion-controlled processes [26,29].

3.3. NR and MV as Redox Mediators for C. pasteurianum DSM 525

We started by testing five concentrations of each mediator: 20.0, 50.0, 75.0, 100.0, and 150.0 µM, under anaerobic conditions (Figure S1 and Figure S2). We selected the highest concentration (150.0 µM) for tests with MFC_{DSM} because it provided optimal *j*-values regardless of the mediator. In addition, preliminary tests had shown that adding 150.0 µM NR or MV does not inhibit *C. pasteurianum* DSM 525 growth (Figure S3).

We selected the potential for recording the amperometric *i-t* curves on the basis of the oxidation potential of each mediator determined by CV. We applied an anodic overpotential (η) of 250 mV. Thus, we measured the current density at a fixed potential of -0.22 V *vs* Ag/AgCl and -0.16 V *vs* Ag/AgCl(sat) for MFC_{DSM} in the presence of NR or MV in the anodic chamber, respectively. Furthermore, we obtained amperometric *i-t* curves for *C. pasteurianum* DSM 525 without a mediator (MFC_{DSM}, control) in the same experimental conditions (Figure 3).

For the electrochemical tests, MFC_{DSM} (*C. pasteurianum* DSM 525, O.D. = 0.2) in the presence of NR or MV in the anodic chamber gave current density of 17.05 ± 2.25 and 8.45 ± 2.98 µA cm^{-2}, respectively. The combined system improved the *C. pasteurianum* DSM 525 catalytic performance by

 doi:10.20944/preprints202409.0776.v1

7.0- and 3.7-fold for NR and MV, respectively, compared to MFC$_{DSM}$ in the absence of a mediator (2.47 ± 0.53 and 2.29 ± 0.69 μA cm^{-2} by applying -0.22 and -0.16 V *vs* Ag/AgCl$_{(sat)}$, respectively).

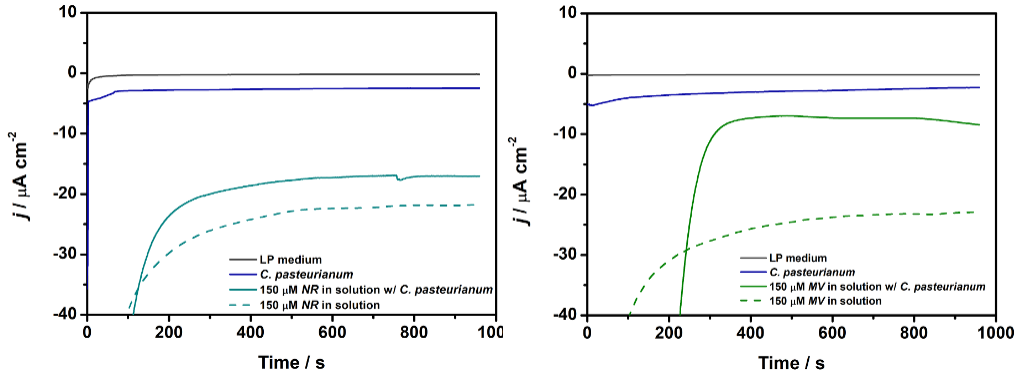

Figure 3. Representative amperometric i-t tests were conducted for (A) NR and (B) MV, in solution at 150.0 μM, in presence and absence of *C. pasteurianum* DSM 525. All experiments were carried out in LP medium (pH = 7) at 25 ± 2 °C.

Introducing mediators can enhance the *C. pasteurianum* DSM 525 EET ability given that the MFC$_{DSM}$ *j*-values improved compared to the abiotic control. Mediators are frequently used with *C. pasteurianum* in traditional fermentation and electrofermentation systems. However, studies focusing on EET enhancement are scarce. Many mediators can alter the NADH/NAD$^+$ redox ratio and modulate the profile of the desired products [30]. This metabolic shift occurs because substrate conversion into products relies on a specific balance between electron donors and acceptors that is unique to each microorganism [31]. Additional research is needed to investigate the use of mediators to facilitate EET in *C. pasteurianum*.

Nevertheless, the presence of *C. pasteurianum* DSM 525 in MFC$_{DSM}$ diminished its *j*-values compared to the presence of a mediator alone in solution (Figure 3). Mediators can form radicals that may react with cellular components, to decrease the electronic efficiency and to increase electronic losses. Conversely, compared to *C. pasteurianum* DSM 525 alone, the catalytic efficiency improved, indicating that the *C. pasteurianum* DSM 525, mediator, and anode interacted.

3.4. FNR or FMV Deposited on the MFC$_{DSM}$ Anode as Mediator

Due to the results obtained in the previous section (3.3), we investigated whether FNR or FMV enhances electron collection in MFC$_{DSM}$. Upon electropolymerization, NR forms poly(neutral red), known as FNR, which is extensively investigated for biosensor applications [25]. As mentioned earlier, FNR can react with biological components (e.g., NADH, proteins, and enzymes) [25].

In turn, immobilized viologen-based mediators have been successfully employed to interact with biological components [27]. However, unlike FNR, FMV interacted weakly with the MFC$_{DSM}$ anodic electrode, so the carbon chain did not increase effectively. This effect has already been described, and the fact that the reduced species MV$^+$ is prone to dimerization has been reported [32].

First, we evaluated the optimal number of CV cycles for FNR and FMV (Figure S4) in the absence of *C. pasteurianum* DSM 525 (abiotic control). In the case of FNR, the current density increased between 10 and 20 cycles and decreased thereafter. Therefore, for FNR, we adopted 20 cycles for FNR in further investigations. Concerning MV, the current density started to decrease after 10 cycles, so we limited assays with FMV to 10 cycles (Figure S5). In the latter case, decreasing current density upon increasing number of cycles was probably due to MV$^+$ species forming dimers, which can further disproportionate into MV^{2+} and insoluble MV^0 [32].

We tested MFC$_{DSM}$ (*C. pasteurianum* DSM 525, O.D. = 0.2) across all CV cycles for each mediator film. The combination of MFC$_{DSM}$ with FNR or FMV increased the current density in all the CV cycles (Figure S6). Nevertheless, although FMV interacted with *C. pasteurianum* DSM 525 on the anode, it did not interact as effectively as FNR.

 doi:10.20944/preprints202409.0776.v1

Figures 4A and B compare the amperometric *i-t* tests for the highest current density achieved with FNR (20 cycles) and FMV (10 cycles), respectively, at MFC$_{DSM}$. After we introduced FNR into the MFC$_{DSM}$ anodic chamber, the current density increased by 12-fold compared to MFC$_{DSM}$ (30.76 ± 3.44 and 2.47 ± 0.53 μA cm^{-2}, respectively). As for FMV, the current density increased by 3.9-fold after it was introduced into the MFC$_{DSM}$ anodic chamber compared to MFC$_{DSM}$ (8.91 ± 1.92 and 2.29 ± 0.69 μA cm^{-2}, respectively)

Regarding FNR introduction into the MFC$_{DSM}$ anodic chamber, the current density doubled compared to NR introduction into the MFC$_{DSM}$ anodic chamber (30.76 ± 3.44 and 17.05 ± 2.25 μA cm^{-2}, respectively). This effect has not been previously reported for *C. pasteurianum* DSM 525. This result suggested that the presence of FNR on the electrode surface enhances the electron collection efficiency and reduces electron losses. In addition, the presence of FNR improves the EET capacity of *C. pasteurianum* DSM 525, indicating that the film interacts with the microorganism.

On the other hand, FMV or MV introduction into the MFC$_{DSM}$ anodic chamber elicited similar effects: 3.9- and 3.7-fold increase in the current density compared to MFC$_{DSM}$. The MV structure does not favor the formation of polymeric films, so MV remains mostly in the dimeric form [32]. The dimer and monomer must diffuse in a similar way, which could explain the similar increase in current density.

We recorded CV curves at 1 mV s^{-1} to determine the anodic peak potentials for each mediated electron transfer system. We conducted the experiments with MFC$_{DSM}$ and FNR or FMV (Figures 4C and D). We also recorded a control CV without the biocatalyst (abiotic control). The data confirmed the results described above that the presence of FNR in the MFC$_{DSM}$ anodic chamber increased the current density, while the presence of FMV in the MFC$_{DSM}$ anodic chamber elicited a less pronounced capacitive behavior.

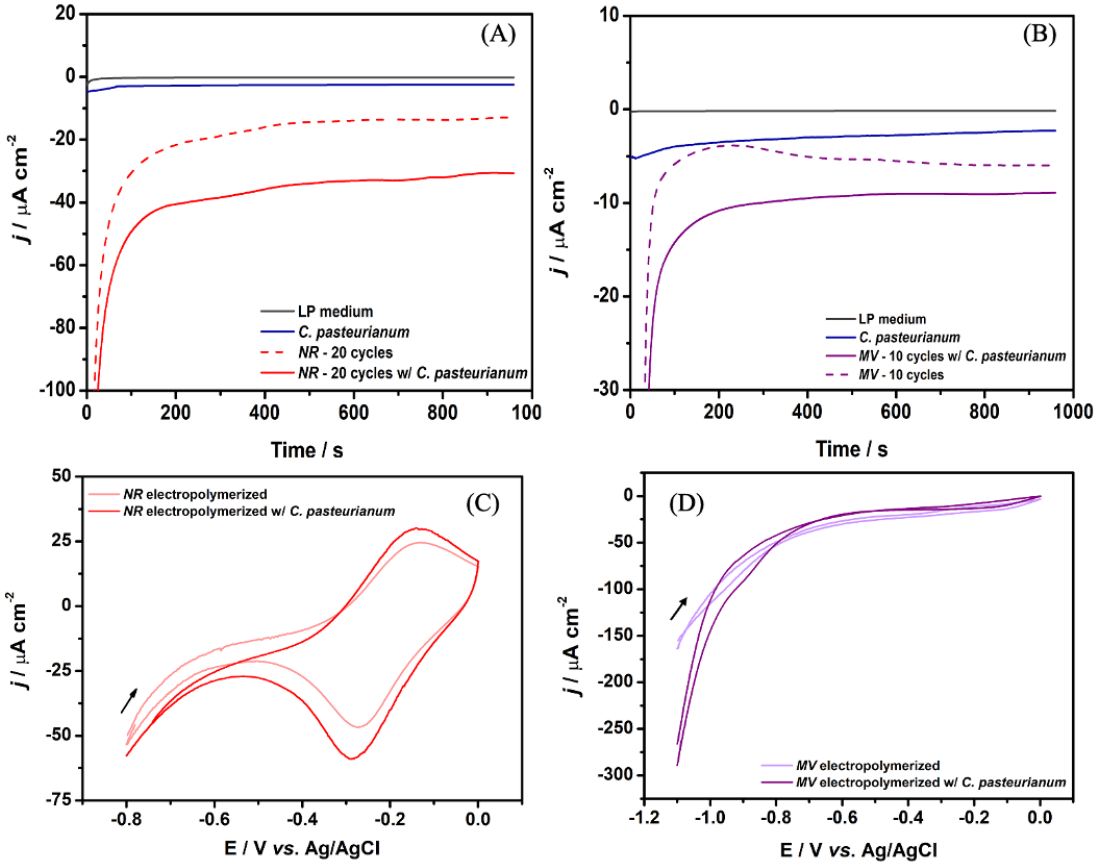

Figure 4. Representative amperometric *i-t* tests were conducted for (A) FNR at 20 cycles and (B) FMV at 10 cycles both in the presence and absence of *C. pasteurinum* DSM 525 (MFC$_{DSM}$ and abiotic control, respectively). CVs comparing the anodic electrodes with (C) FNR and with or without *C. pasteurinum* DSM 525 (MFC$_{DSM}$ and abiotic control, respectively) at 20 cycles and (D) FMV and with or without *C.*

 doi:10.20944/preprints202409.0776.v1

pasteurinum DSM 525 (MFC_{DSM} and abiotic control, respectively) at 10 cycles (scan rate of 1 mV s^{-1}). All the experiments were carried out in LP medium (pH = 7) at 25 ± 2 °C.

Figure S7 compares the EIS of the unmodified electrode (carbon cloth) and the modified electrode containing FNR and FMV. In the two latter cases, total impedance decreased significantly. Specifically, containing FNR and FMV had R_{ct} of 30.4 and 48.3 Ω, respectively, which represent 33.7- and 21.4-fold reduction compared to unmodified electrode (R_{ct} = 1025.6 Ω). As for R_s, values were similar (20.5, 18.3, and 21.7 Ω for unmodified electrode, containing FNR, and containing FMV, respectively).

4. Conclusions

We investigated C. pasteurianum DSM 525 as a biocatalyst in the anode of an MFC. Although the genus Clostridium commonly occurs in bioanodes, its EET capacity is not fully understood. In the presence of this biocatalyst, the MFC current output almost doubled (1.72 vs 3.02 μA cm^{-2}), which evidenced direct EET. The EET capacity can be further enhanced by introducing NR or MV as a mediator into the MFC_{DSM}, either in solution or as a film (FNR and FMV, respectively). Compared to NR, FNR introduction into the MFC_{DSM} produced almost twice the current density (17.05 ± 2.25 vs 30.76 ± 3.44 μA cm^{-2}). Conversely, introduction of MV or FMV into the MFC_{DSM} produced nearly identical current density (8.45 ± 2.98 vs 8.91 ± 1.92 μA cm^{-2}), indicating that FMV was a less effective mediator than FNR. Therefore, FMV might interact weakly with the MFC_{DSM} anode, possibly due to dimer formation. In turn, FNR appears to be promising to enhance C. pasteurianum DSM 525 EET because it potentially facilitates microorganism-film-anode interaction.

Supplementary Materials: The following supporting information can be downloaded at the website of this paper posted on Preprints.org, Figure S1: Representative amperometric i-t tests conducted for (A) NR and(B) MV mediators in the solution at different concentrations. All experiments were carried out in LP medium (pH = 7) at 25 ± 2 °C. An overpotential of 250 mV was applied over the anodic peak indicated by CV.; Figure S2: Comparison of current densities of NR and MV at concentrations of 20.0, 50.0, 75.0, 100.0, and 150.0 μM.; Figure S3: O.D. at 600 nm taken over 16 hours to monitor the growth of *C. pasteurianum* DSM 525 in the presence of NR and MV at 150.0 μM. A control experiment was conducted with only with DSM 525, excluding any mediators.; Figure S4: Optimization of the number of electropolymerization cycles for (A) NR and (B) MV by amperometric i-t tests in LP medium (pH 7.0), at 25 ± 2 °C.; Figure S5: Cyclic voltammograms (CVs) of electropolymerization for (A) NR and (B) MV.; Figure S6: Representative amperometric i-t tests were conducted for (A) NR and (B) MV in presence and absence of C. pasteurianum DSM 525 across different electropolymerization cycles. All experiments were carried out in LP medium (pH =7) at 25 2 °C. An overpotential of 250 mV was applied over the anodic peak indicated by CV.; Figure S7: EIS at fixed potential for (A) the electrode modified with FNR (-0.22V-red line) and (B) FMV (-0.16 V- purple line) at 20 and 10 cycles, respectively. (black line) blank experiment in absence of electromediated film.

Author Contributions: Conceptualization, A.C.B.Z. and V.R.; methodology, A.C.B.Z., J.C.Z., A. R. d. A. and V.R.; investigation, A.C.B.Z. and J.C.S.; resources, A. R. d. A. and V.R.; data acuration, A.C.B.Z., J.C.Z., A. R. d. A. and V.R.; writing—original draft preparation, A.C.B.Z., A. R. d. A. and V.R.; writing—review and editing, A.C.B.Z., A. R. d. A. and V.R.; supervision, A. R. d. A. and V.R.

Funding: The authors are grateful to the São Paulo State Research Foundation (FAPESP, grant numbers 2024/00725-0, 2022/04024-0, 2021/12866-9, 2023/07992-0), and the National Institute for Alternative Technologies of Detection, Toxicological Evaluation and Removal of Micropollutants and Radioactives (INCT-DATREM, grant numbers FAPESP 2014/50945-4, CNPq 465571/2014-0) for financial support.

Institutional Review Board Statement: Not applicable.

Informed Consent Statement: Not applicable.

Data Availability Statement: Data are contained within the article and Supplementary Materials. .

Acknowledgments: To Cynthia Maria de Campos Prado Manso for review of the English language.

Conflicts of Interest: The authors declare no conflicts of interest.

References

1. Simoska, O.; Gaffney, E. M.; Lim, K.; Beaver, K.; Minteer, S. D. Understanding the Properties of Phenazine Mediators that Promote Extracellular Electron Transfer in Escherichia coli. *J. Electrochem. Soc.* 2021, 168(2), 25503. https://doi.org/10.1149/1945-7111/abe52d
2. Zhang, S.; You, J.; Chen, H.; Ye, J.; Cheng, Z.; Chen, J. Gaseous toluene, ethylbenzene, and xylene mixture removal in a microbial fuel cell: Performance, biofilm characteristics, and mechanisms. *Chem. Eng. J.* 2020, *386*, 123916. https://doi.org/10.1016/j.cej.2019.123916.
3. Lim, C. E.; Chew, C. L.; Pan, G.-T.; Chong, S.; Arumugasamy, S. K.; Lim, J. W.; Al-Kahtani, A. A.; Ng, H.-S.; Abdurrahman, M. Predicting microbial fuel cell biofilm communities and power generation from wastewaters with artificial neural network. *Int. J. Hydrog. Energy*, 2024, *52*, 1052–1064. http://dx.doi.org/10.1016/j.ijhydene.2023.08.290.
4. Logan, B.E. Microbial Fuel Cells. John Wiley & Sons, Inc., New York, 2008.
5. Paquete, C. M. Electroactivity across the cell wall of Gram-positive bacteria. *Comput. Struct. Biotechnol. J.* 2020, 18, pp. 3796–3802. https://doi.org/10.1016/j.csbj.2020.11.021.
6. Mancílio, L. B. K.; Ribeiro, G. A.; Lopes, E. M., Kishi; L. T., Martins-Santana, L.; de Siqueira, G. M. V.; Andrade, A. R.; Guazzaroni, M.-E.; Reginatto, V. (2020). Unusual microbial community and impact of iron and sulfate on microbial fuel cell ecology and performance. *Curr. Res. Biotechnol*. 2020, *2*, pp. 64–73. http://dx.doi.org/10.1016/j.crbiot.2020.04.001.
7. Park, H. S.; Kim, B. H.; Kim, H. S.; Kim, H. J.; Kim, G. T.; Kim, M.; Chang, I. S.; Park, Y. K.; Chang, H. I. A novel electrochemically active and Fe(III)-reducing bacterium phylogenetically related to *Clostridium butyricum* isolated from a microbial fuel cell. Anaerobe, 2001, 7(6), pp. 297–306. https://doi.org/10.1006/anae.2001.0399.
8. dos Passos, V. F.; Marcilio, R.; Aquino-Neto, S.; Santana, F. B.; Dias, A. C. F.; Andreote, F. D.; de Andrade, A. R.; Reginatto, V. Hydrogen and electrical energy co-generation by a cooperative fermentation system comprising *Clostridium* and microbial fuel cell inoculated with port drainage sediment. *Bioresour. Technol.* 2019, *277*, pp. 94–103. https://doi.org/10.1016/j.biortech.2019.01.031.
9. Choi, O.; Kim, T.; Woo, H. M.; Um, Y. Electricity-driven metabolic shift through direct electron uptake by electroactive heterotroph *Clostridium pasteurianum*. *Sci. Rep.* 2014, *4*, 6961. https://doi.org/10.1038/srep06961.
10. Beaver, K.; Dantanarayana, A.; Zani, A. B.; Lehto, D. L.; Minteer, S. D. Nitric Oxide as a Signaling Molecule for Biofilm Formation and Dispersal in Mediated Electron Transfer Microbial Electrochemical Systems. *J. Electrochem. Soc.* 2023, *170*(4), 045503. https://doi.org/10.1149/1945-7111/acc97e.
11. Hassan, R. Y. A.; Febbraio, F.; Andreescu, S. Microbial Electrochemical Systems: Principles, Construction and Biosensing Applications. *Sensors*, 2021, *21*(4), 1279. https://doi.org/10.3390/s21041279.
12. Zani, A. C. B.; de Almeida, É. J. R.; Furlan, J. P. R.; Pedrino, M.; Guazzaroni, M.-E.; Stehling, E. G.; de Andrade, A. R.; Reginatto, V. Electrobiochemical skills of *Pseudomonas aeruginosa* species that produce pyocyanin or pyoverdine for glycerol oxidation in a microbial fuel cell. *Chemosphere*, 2023, *335*, 139073. https://doi.org/10.1016/j.chemosphere.2023.139073.
13. Marsili, E.; Baron, D. B.; Shikhare, I. D.; Coursolle, D.; Gralnick, J. A.; Bond, D. R. *Shewanella* secretes flavins that mediate extracellular electron transfer. *Proc. Natl. Acad. Sci.* 2008, 105 (10), pp. 3968-3973. https://doi.org/10.1073/pnas.0710525105.
14. Grattieri, M.; Rhodes, Z.; Hickey, D. P.; Beaver, K.; Minteer, S. D. Understanding Biophotocurrent Generation in Photosynthetic Purple Bacteria. *ACS Catal.* 2019, *9*(2), pp. 867–873. http://dx.doi.org/10.1021/acscatal.8b04464.
15. de Lacey, A. L.; Bes, M. T.; Gómez-Moreno, C.; Fernández, V. M. Amperometric enzyme electrode for NADP+ based on a ferrodoxin-NADP+ reductase and viologen-modified glassy carbon electrode. *J. Electroanal. Chem.* 1995, *390*(1), pp. 69–76. https://doi.org/10.1016/0022-0728(95)03898-Q.
16. Lovley, D. R.; Phillips, E. J. P. Novel Mode of Microbial Energy Metabolism: Organic Carbon Oxidation Coupled to Dissimilatory Reduction of Iron or Manganese. *Appl. Environ. Microbiol*. 1998, 54 (6), pp. 1472-1480. https://doi.org/10.1128%2Faem.54.6.1472-1480.1988.
17. Arechederra, R. L.; Minteer, S. D. Complete Oxidation of Glycerol in an Enzymatic Biofuel Cell. *Fuel Cells*, 2009, *9*(1), pp. 63–69. https://doi.org/10.1002/fuce.200800029.
18. Guynn, I. P. A.; Beaver, K.; Gaffney, E. M.; Zani, A. B.; Dantanarayana, A.; Minteer, S. D. *Salinivibrio* sp. EAGSL as a halophilic and ectoine-producing bacteria for broad microbial electrochemistry applications. *Cell Reports Physical Science*. 2023, *4*(6), 101420. https://doi.org/10.1016/j.xcrp.2023.101420.
19. Ghica, M.; Brett, C. Glucose oxidase inhibition in poly(neutral red) mediated enzyme biosensors for heavy metal determination. *Mikrochim. Acta*. 2008, *163*, pp. 185–193. http://dx.doi.org/10.1007/s00604-008-0018-1.
20. Kumar, S. S.; Malyan, S. K.; Basu, S.; Bishnoi, N. R. Syntrophic association and performance of *Clostridium*, *Desulfovibrio*, *Aeromonas* and *Tetrathiobacter* as anodic biocatalysts for bioelectricity generation in dual chamber microbial fuel cell. *Environ. Sci. Pollut. Res.* 2017, *24*(19), pp. 16019–16030. https://doi.org/10.1007/s11356-017-9112-4.

21. Taufemback, W. F.; Hotza, D.; Recouvreux, D. de O. S.; Calegari, P. C.; Pineda-Vásquez, T. G.; Antônio, R. V.; Watzko, E. S. Techniques for obtaining and mathematical modeling of polarization curves in microbial fuel cells. *Mater. Chem. Phys.* 2024, 315, 128998. https://doi.org/10.1016/j.matchemphys.2024.128998.
22. Boas, J. V.; Oliveira, V. B.; Simões, M.; Pinto, A. M. F. R. Review on microbial fuel cells applications, developments and costs. *J. Environ. Manage.* 2022, *307*, 114525. https://doi.org/10.1016/j.jenvman.2022.114525.
23. Souza, J. C.; Machini, W. B. S.; Zanoni, M. V. B.; Oliveira-Brett, A. M. Human Hair Keratin Direct Electrochemistry and In Situ Interaction with *p*-Toluenediamine and p-Aminophenol Hair Dye Precursors using a Keratin Electrochemical Biosensor. *ChemElectroChem*, 2020, *7*(5), pp. 1277–1285. https://doi.org/10.1002/celc.202000151.
24. Rhodes, Z.; Simoska, O.; Dantanarayana, A.; Stevenson, K. J.; Minteer, S. D. Using structure-function relationships to understand the mechanism of phenazine-mediated extracellular electron transfer in *Escherichia coli*. *IScience*. 2021, *24*(9), 103033. https://doi.org/10.1016/j.isci.2021.103033.
25. Pauliukaite, R.; Ghica, M.E.; Barsan, M.; Brett, C. M. A. Characterisation of poly(neutral red) modified carbon film electrodes; application as a redox mediator for biosensors. *J Solid State Electrochem*. 2007, 11, pp. 899–908. http://dx.doi.org/10.1007/s10008-007-0281-9.
26. *Bard,A.J.; Faulkner, L.R. Electrochemical Methods*: *Fundamentals and Applications*. *2nd Edition*, John *Wiley* & Sons, *New York*, *2001*.
27. Ghica, M. E.; Brett, C. M. A. A glucose biosensor using methyl viologen redox mediator on carbon film electrodes. *Anal. Chim. Acta*. 2005, *532*(2), pp. 145–151. https://doi.org/10.1016/j.aca.2004.10.058.
28. Peguin, S.; Goma, G.; Delorme, P.; Soucaille, P. Metabolic flexibility of *Clostridium acetobutylicum* in response to methyl viologen addition. *Appl Microbiol Biotechnol*. 1994, 42, pp. 611–616. https://doi.org/10.1007/BF00173928.
29. Shpilevaya, I.; Foord, J. S. Electrochemistry of Methyl Viologen and Anthraquinonedisulfonate at Diamond and Diamond Powder Electrodes: The Influence of Surface Chemistry. *Electroanalysis*, 2014, *26*(10), pp. 2088–2099. https://doi.org/10.1002/elan.201400310.
30. He, A.-Y.; Yin, C.-Y.; Xu, H.; Kong, X.-P.; Xue, J.-W.; Zhu, J.; Jiang, M.; Wu, H. Enhanced butanol production in a microbial electrolysis cell by *Clostridium beijerinckii* IB4. *Bioproc. Biosyst. Eng.* 2016, *39*(2), pp. 245–254. https://doi.org/10.1007/s00449-015-1508-2.
31. Martínez-Ruano, J.; Suazo, A.; Véliz, F.; Otálora, F.; Conejeros, R.; González, E.; Aroca, G. Electro-fermentation with *Clostridium autoethanogenum*: Effect of pH and neutral red addition. *Environ. Technol. Inno.* 2023, *31*, 103183. https://doi.org/10.1016/j.eti.2023.103183.
32. Liu, Y.; Chen, Q.; Zhang, X.; Ran, J.; Han, X.; Yang, Z.; Xu, T. Degradation of electrochemical active compounds in aqueous organic redox flow batteries. *Curr. Opin. Electroche.* 2022, 32, 100895. https://doi.org/10.1016/j.coelec.2021.100895.